Annual Review of Vision Science

Topographic Variations in Retinal Encoding of Visual Space

Alina Sophie Heukamp,* Rebekah Anne Warwick,* and Michal Rivlin-Etzion

Department of Neurobiology, Weizmann Institute of Science, Rehovot 7610001, Israel; email: alina.heukamp@weizmann.ac.il, rebekah.warwick@weizmann.ac.il, michal.rivlin@weizmann.ac.il

Annu. Rev. Vis. Sci. 2020. 6:1.1–1.23

The *Annual Review of Vision Science* is online at vision.annualreviews.org

https://doi.org/10.1146/annurev-vision-121219-081831

*These authors contributed equally to this article

Keywords

retina, fovea, mouse, retinal ganglion cells, topography, cone opsins

Abstract

A retina completely devoid of topographic variations would be homogenous, encoding any given feature uniformly across the visual field. In a naive view, such homogeneity would appear advantageous. However, it is now clear that retinal topographic variations exist across mammalian species in a variety of forms and patterns. We briefly review some of the more established topographic variations in retinas of different mammalian species and focus on the recent discovery that cells belonging to a single neuronal subtype may exhibit distinct topographic variations in distribution, morphology, and even function. We concentrate on the mouse retina—originally viewed as homogenous—in which genetic labeling of distinct neuronal subtypes and other advanced techniques have revealed unexpected anatomical and physiological topographic variations. Notably, different subtypes reveal different patterns of nonuniformity, which may even be opposite or orthogonal to one another. These topographic variations in the encoding of visual space should be considered when studying visual processing in the retina and beyond.

1. INTRODUCTION

Retinal neurons: neurons composing five major groups, photoreceptors, bipolar cells, retinal ganglion cells, horizontal cells, and amacrine cells

Cell subtype: each cell type is comprised of subtypes, and neurons of the same subtype are expected to have similar characteristics

Photoreceptors: the light-sensitive neurons of the retina, made up of two types, rods and cones for night and day vision, respectively

The retina is a thin neuronal layer that lines the back of the eye. The visual field is focused via the eye's optics as a two-dimensional image onto the entire retinal area. In a naive view, we would expect the retina to be homogenous, so that any given feature in the visual field is equally represented at any given location. This assumption has given rise to the mosaic concept, in which any given subtype of retinal neuron would be arranged in the retina with regular distances between cell bodies (Masland 2012, Rodieck 1991, Wässle 2004). This regular spacing between cells of a single subtype would allow equal representation of a specific visual feature across the retina while preventing redundancy resulting from overlaps. Nevertheless, topographic variations in the retina have long been recognized, and specialized regions for higher spatial acuity were detected in numerous species (e.g., human fovea). It is currently believed that specialized regions can arise in different forms, and thus that cells belonging to a single neuronal subtype may exhibit nonuniform distributions, variations in morphology, and even variations in physiology across the retina.

Below, we describe some of the well-established topographic variations in the distribution and morphology of neurons in the primate retina and discuss recently discovered variations in their function. We then discuss topographic variations in spectral sensitivity found across a large variety of species. We focus on the mammalian retina, giving examples of interspecies variations and speculating on their roles. Lastly, we concentrate on the mouse, which has become a popular model organism in visual neuroscience (Huberman & Niell 2011). The mouse retina was originally viewed as homogenous, lacking any significant topographic variation (Dräger & Olsen 1981, Jeon et al. 1998), but genetic labeling of distinct retinal cell subtypes has recently revealed that topographic variations do exist in distribution, morphology, and even function. Notably, the different cell subtypes do not necessarily reveal the same topographic variation. Based on the unique topographic variations of each cell subtype and their hypothesized roles in mouse vision, we suggest potential benefits for the mouse resulting from its retinal inhomogeneity.

2. RETINAL SPECIALIZATIONS: FOVEA, VISUAL STREAK, AND AREA CENTRALIS

One specific retinal topographic variation, namely the fovea, was described over 150 years ago in the human retina (Chievitz 1889, Müller 1861). The fovea has a small area (approximately 0.8–1.5 mm in diameter in humans) that usually lacks rod photoreceptors and in which cone photoreceptors are densest and have elongated outer segments (Hendrickson 2005, Polyak 1941, Walls 1942). It is characterized by a lateral displacement of cells from the inner retinal layers, resulting in minimal light scattering (Polyak 1957) (**Figure 1*a***). Foveae are found in humans and some other primates, as well as reptiles and birds. Some species, primarily birds, have two foveae: one in the temporal region, serving binocular vision, and another in the nasal region, serving monocular vision (Bringmann et al. 2018, Moroney & Pettigrew 1987). The fovea, on which we elaborate in Section 3, underlies visual-based behaviors that require the highest spatial acuity, such as reading in humans and detection of small animals from large distances in birds of prey.

Other specialized retinal regions with higher concentrations of cones compared to neighboring areas were later found in various species in different forms. These, like the fovea, serve to enhance spatial acuity in specific parts of the visual field. We briefly present these retinal specializations, which have also been extensively covered elsewhere (Ahnelt & Kolb 2000, Bringmann et al. 2018, Hauzman et al. 2018, Moore et al. 2017).

A visual streak is an elongated region of increased cell density. Most visual streaks span along the naso-temporal retinal axis and are found in many carnivores, as well as in the rabbit, pig, gray

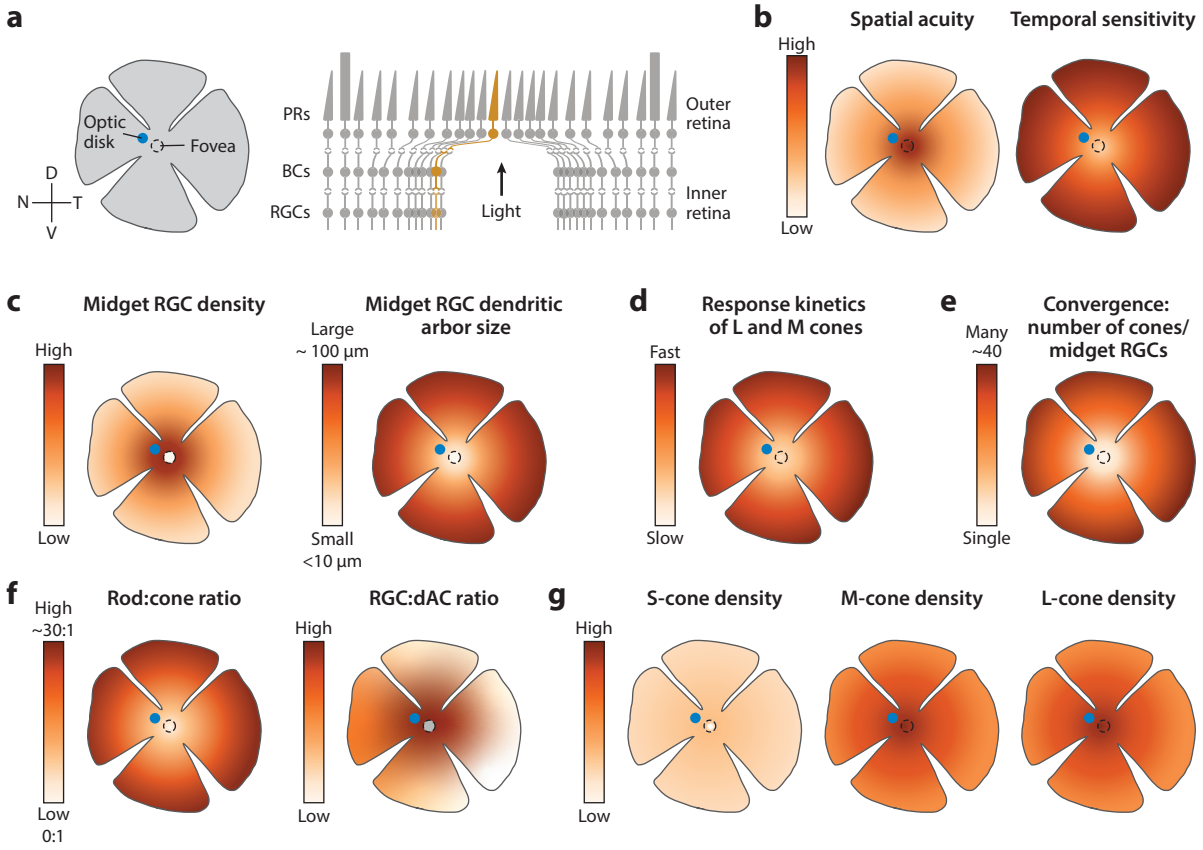

Figure 1

Topographic variations in the primate retina. (*a*, *left*) Schematic view of a primate retina labeling fovea (*black dashed circle*) and optic disk (the exit point of the optic nerve) (*blue spot*). For better visibility, the size of the fovea has been increased and is therefore not to scale. (*Right*) Schematic cross-section through a fovea showing photoreceptors (PRs), bipolar cells (BCs), and retinal ganglion cells (RGCs). An example of a private line from one cone to one midget RGC is labeled in orange. Note the lateral displacement of all cells except for cones from the central fovea. (*b*) Schematic colormaps representing spatial acuity (*left*) and temporal sensitivity (*right*) across the retina. (*c*) Schematic colormaps representing the density (*left*) and dendritic arbor size (*right*) of midget RGCs. (*d*) Schematic colormap representing response kinetics of L and M cones. (*e*) Schematic colormaps showing the convergence of the number of cones onto one midget RGC. (*f*) Schematic colormaps showing rod:cone ratio (*left*) and RGC:displaced amacrine cell (dAC) ratio (*right*). (*g*) Schematic colormaps showing the densities of S (*left*), M (*middle*), and L cones (*right*).

kangaroo, and other species (Hughes 1975, Levick 1967, Schiviz et al. 2008). According to Hughes' terrain theory, such visual streaks are most beneficial for terrestrial animals inhabiting open fields, as they provide a panoramic view of the horizon that does not require eye or head movement, facilitating location of prey and detection of an approaching predator (Collin 2008, Hughes 1977). Less common are the vertical streaks that span along the dorso-ventral axis. These serve species whose visual field is dominated by vertically oriented features, such as the tree branches seen by the sloth (Andrade-de-Costa et al. 1989) or the trunk of the African elephant (Stone & Halasz 1989).

The area centralis is a circular region of increased cell density, usually located in the temporal retina and thus included in the frontal binocular visual field (Hauzman et al. 2018). Animals with an area centralis use eye and head movements to focus different parts of the image onto this area to

increase spatial resolution. An area centralis is often found in arboreal species (e.g., tree kangaroo, most primates, opossum), whose fields of view are normally obscured by nearby vegetation (Schiviz et al. 2008). Note that, in some cases in the literature, the fovea and the visual streak are referred to as specialized forms of an area centralis.

Retinal ganglion cells (RGCs): output neurons that send axons to higher-order brain areas; each RGC encodes a different modality in the visual field

Overall, the presence of retinal specializations does not seem to be phylogenetically determined, but rather evolved to meet environmental requirements of higher visual acuity in specific areas of the visual field.

3. FUNCTIONAL DIFFERENCES FROM FOVEA TO PERIPHERY IN THE PRIMATE RETINA

It is well established that the primate retina is inhomogeneous in terms of spatial resolution, as spatial visual acuity is highest in the fovea and sharply decreases with retinal eccentricity (Bringmann et al. 2018, Moore et al. 2017) (**Figure 1*b***). The high spatial resolution in the fovea is derived from the high density of cone photoreceptors and downstream midget retinal ganglion cells (RGCs) (Hirsch & Curcio 1989, Wässle et al. 1989) (**Figure 1*c***). Midget RGCs comprise approximately 80% of foveal RGCs, and their small dendritic arbors [<10 μm in diameter in the human fovea (Kolb & Marshak 2003)] are crucial for the high spatial acuity. In the fovea, each midget cell gathers input from only one bipolar cell that gets its input from only one cone, forming a private line (**Figure 1*a***) from a single cone to higher-order brain areas (Calkins et al. 1994, Kolb & Dekorver 1991) (**Figure 1*e***). Outside the fovea, spatial resolution decreases in accordance with the decreased density of midget RGCs and the increase in their dendritic arbor size and resultant cone sampling (Dacey & Petersen 1992, Field et al. 2010, Kolb & Marshak 2003, Rossi & Roorda 2010, Wässle et al. 1989) (**Figure 1*c***). In the far peripheral retina, midget RGCs can have dendritic arbor sizes as large as 100 μm (Dacey & Petersen 1992, Watanabe & Rodieck 1989) and collect inputs from approximately 40 cones (Goodchild et al. 1996) (**Figure 1*c*,*e***), losing the fine spatial resolution of their counterparts in the fovea in favor of increased contrast sensitivity (Goodchild et al. 1996).

Temporal sensitivity also varies across the retina, but in an apparently opposite pattern to that of the spatial resolution: Psychophysical measurements showed that the critical flicker frequency (CFF)—the frequency at which a flickering light appears steady—is higher in the periphery than in the center of the visual field (Hecht & Verrijp 1933, Rovamo & Raninen 1988, Tyler 1985, Waugh & Hess 1994) (**Figure 1*b***). While the variations in temporal sensitivity could arise in higher visual processing stages, several studies found that they have an outer retinal origin. First, focal electroretinogram (ERG) recordings also showed an increase in the CFF as a function of retinal eccentricity (Seiple & Holopigian 1996). Second, in vivo recordings from macaque retina showed that both midget and parasol RGCs display eccentricity-dependent increases in CFF (Solomon et al. 2002). Recently, Sinha and colleagues (2017) used an in vitro whole-mount retinal preparation to establish the mechanisms underlying temporal differences between foveal and peripheral midget RGCs. They found that response kinetics (assessed by time to peak) gradually changed with retinal eccentricity, being approximately twofold slower in the fovea than in the periphery. They also found remarkable circuit differences across retinal regions, as inhibitory inputs to midget RGCs were negligible in the fovea but robust in the periphery. Because inhibition plays a crucial role in shaping neuronal circuit computations (Isaacson & Scanziani 2011), one could hypothesize that the differential inhibition would lead to different response kinetics between fovea and periphery. Surprisingly, this assumption was found to be wrong. Dynamic clamp recordings from foveal and peripheral midget RGCs demonstrated that their response kinetics were dominated by the cells' excitatory rather than inhibitory input. Moreover, a foveal and a

peripheral midget cell injected with the same currents responded similarly (Sinha et al. 2017). Accordingly, kinetics of excitatory inputs to midget RGCs vary with retinal eccentricity. To resolve the source of the differences in excitatory inputs, cone inner segment voltages were recorded at different retinal eccentricities. Light-dependent voltage changes of L and M cones were twofold slower in the fovea than in the periphery, comparable to the differences observed between foveal and peripheral midget RGCs (Sinha et al. 2017) (**Figure 1*d***). These data together demonstrate that cone photoreceptors directly contribute to the variation in temporal sensitivity in the primate retina. The temporal differences may be further enhanced by differences in the underlying circuits, for example, by the number of cells converging onto an RGC, which increases with eccentricity.

These findings have major implications for our understanding of the primate retina, as they imply that visual processing in the fovea and the periphery do not merely differ by a convergence factor, but rather have different computational roles that are implemented by distinct neuronal circuits. Further evidence supports the distinction between fovea and periphery. Rods avoid the fovea but outnumber cones in the peripheral retina, reaching a rod:cone ratio of 30:1 in certain areas (Curcio et al. 1990) (**Figure 1*f***). The inhomogeneous rod:cone ratio supports photopic vision in the fovea and scotopic vision in the periphery, but it may have other functional implications: Studies in rodents and other mammals demonstrated that signals originating in the rod photoreceptors traverse the retina through three parallel pathways (Demb & Singer 2012, Grimes et al. 2018), two of which have been suggested to exist in humans (Sharpe & Stockman 1999; but see Grimes et al. 2018). The different retinal pathways interact extensively via lateral connections mediated by horizontal and amacrine cells and contribute to the complexity of retinal computations (Rivlin-Etzion et al. 2018). Accordingly, the percentage of displaced amacrine cells drastically differs across retinal areas. In the central primate retina, only 5% of all neurons in the ganglion cell layer are amacrine cells, but in the far periphery, they comprise nearly 80% of the neurons (Curcio & Allen 1990, Wässle et al. 1989). These results are further supported by gene expression data of amacrine cells, where some subtypes appear to be periphery specific (Peng et al. 2019), and are in line with the weak and strong inhibitory input to foveal and peripheral midget RGCs, respectively (Sinha et al. 2017).

The primate retina displays topographic variations not only with retinal eccentricity, but also across the main vertical and horizontal axes. The most pronounced variation was reported for RGCs along the naso-temporal axis. Ganglion cell density in the peripheral nasal retina was estimated to be 3–8-fold higher than in the corresponding eccentricities in the temporal retina (Curcio & Allen 1990, Perry & Cowey 1985, Wässle et al. 1989). This anisotropy is not shared among all retinal cells. As noted above, the density of displaced amacrine cells is point symmetric and increases with retinal eccentricity only. As a result, in most peripheral areas, the number of displaced amacrine cells exceeds the number of ganglion cells by a factor of five, but in the peripheral nasal retina, ganglion cells outnumber displaced amacrine cells (Wässle et al. 1989) (**Figure 1*f***). The nasal retina processes visual information from the monocular field of view. Thus, the higher ganglion cell density and the increased ganglion:amacrine cell ratio may compensate for the single eye representation and increase spatial resolution.

Inhibition boosts complexity of computations in neuronal circuits in general and underlies the diversity of computational specializations in the retina (Farrow et al. 2013, Franke et al. 2017, Mauss et al. 2017, Münch et al. 2009, Wei 2018). Taken together, the evidence suggests that visual processing in the fovea is inherently different from that in the periphery. While the fovea—poor in rods and amacrine cells—carries out simple processing, the periphery (and, to a lesser degree, the nasal periphery)—rich in rods and inhibitory neurons—conducts complex computations in response to visual input.

Photopic vision: vision under high-light conditions (usually daylight) mediated by cones

Scotopic vision: vision under low-light conditions (usually nightlight) mediated by rods

Displaced amacrine cells: amacrine cells (mainly inhibitory interneurons) located in the ganglion cell layer of the retina

4. TOPOGRAPHIC VARIATIONS OF CONES IN MAMMALS

Opsin: a protein that becomes light sensitive upon binding to a chromophore and initiates the phototransduction cascade; different opsins have different spectral sensitivities

Center-surround: opposing response to stimuli in center and surround of a neuron's receptive field (e.g., light increments versus decrements, green versus red)

Color vision is based on different types of cone photoreceptors that have different spectral sensitivities. In mammals, the spectral tuning of photoreceptors is determined by the opsin that they express (Baden & Osorio 2019). Since cone responses depend not only on the spectral composition of light but also on photon density, the neural code for color cannot rely on single cones. Color coding arises from a comparison of signals between two or more cone types. This interaction is typically antagonistic and is referred to as color opponency (Dacey & Packer 2003). As color processing depends on intermixing cone signals, the different cone types are expected to present similar densities across the retina, so that the ratio between them is fixed. However, there is ample evidence that argues against this idea, revealing that distinct cone types display different and uncorrelated density functions.

Humans and old world primates exhibit trichromatic color vision, which is based on three cone types with peak sensitivities to long (L cone, approximately 563 nm), middle (M cone, approximately 534 nm), and short (S cone, approximately 420 nm) wavelengths (Bowmaker & Dartnall 1980). While L and M cones, which comprise 90–95% of the cone population, are distributed across the entire retina (Roorda & Williams 1999), S cones avoid a region of approximately 0.25° in the central fovea (Bumsted & Hendrickson 1999, Curcio et al. 1991, de Monasterio et al. 1985, Martin & Grünert 1999, Williams et al. 1981) (**Figure 1*g***). In this central region, color vision is based on chromatic opponency of midget RGCs, whose receptive field center is determined by a single L or M cone through one midget bipolar cell (Calkins et al. 1994, Kolb & Dekorver 1991). Given that the receptive field surround is generated by random cone connectivity, the single cone center excitation would cancel the inhibitory surround from the same cone type, leaving antagonistic L–M inputs (known as the red–green opponency) (Lennie et al. 1991). Beyond this central region, S cones contribute to the neural color code by forming an S versus L + M antagonistic center-surround on distinct RGCs (known as the blue–yellow opponency) (Dacey et al. 2014). Color coding and its underlying circuits continue to vary with retinal eccentricity, as the size of dendritic arbors of midget RGCs increases toward the retinal periphery and inputs from multiple cones of different spectral sensitivities converge to form the receptive field center of a single RGC (for reviews, see Dacey & Packer 2003, Dacey et al. 2014). Thus, color processing in the trichromatic primate retina displays a topographic variation that depends on cone distribution and on receptive field sizes of midget RGCs.

Most mammals are dichromatic, having only two types of cone photoreceptors, with M cone peak spectral sensitivity in the green range (500–530 nm) and S cone peak spectral sensitivity in the blue range (430 nm) (Jacobs 1993). Even rodents, which were considered color blind until three decades ago (Jacobs & Neitz 1989, Neitz & Jacobs 1986), were shown to exhibit two spectral sensitivities that peak in the green range and, surprisingly, in the UV range of the spectrum (Jacobs et al. 1991). These findings were supported by immunocytochemistry, which demonstrated expression of middle-to-long-wavelength-sensitive (M) and short-wavelength-sensitive (S) cone visual pigments in rodents (Govardovskii et al. 1992, Szél & Röhlich 1992).

Subsequent studies by Szél, Röhlich, and their colleagues focused on the mouse retina and made two unexpected discoveries. First, Röhlich et al. (1994) reported the simultaneous expression of two visual pigments in the cone outer segment. These findings were also confirmed in rabbit and guinea pig (Röhlich et al. 1994) and were supported by other studies, proving wrong the accepted dogma that one cone must contain only one visual pigment (Szél et al. 2000). Second, Szél et al. (1992) and Wang et al. (1992) demonstrated for the first time that the two cone opsins can display distinct topographies: In the mouse retina, middle-wavelength-sensitive opsins dominate the dorsal retina, whereas short-wavelength-sensitive opsins dominate in the ventral retina (**Figure 2*a***), forming opposite gradients of green and UV opsin expression.

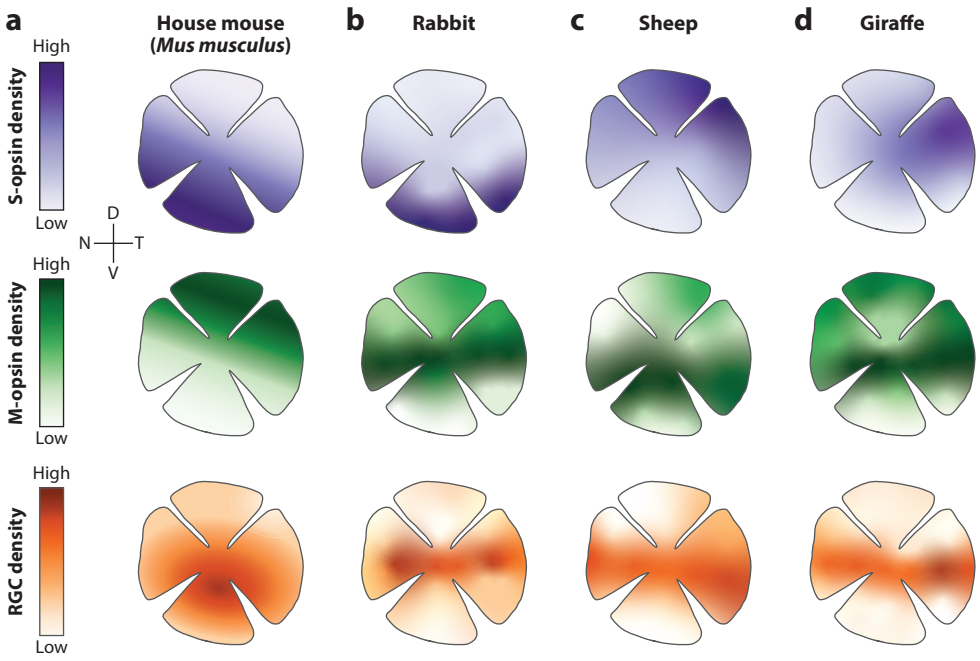

Figure 2

Distribution of S and M opsins in cones across the retina for different mammalian species organized by their height. (*a–d*) Schematic representation of the normalized S opsin (*top*), M opsin (*middle*), and RGC (*bottom*) densities across the retina for (*a*) house mouse (*Mus musculus*), (*b*) rabbit, (*c*) sheep, and (*d*) giraffe.

The discovery that the distribution of cone visual pigments in the mouse differs in the dorsal and ventral regions led researchers to investigate the distribution of cone opsins in other mammalian species. The vast majority of species studied displayed an overall dominance of M over S opsins, with a common ratio of 10:1 or even higher (Szél et al. 2000). The distribution of M opsins tends to correlate with that of RGCs, peaking in areas of higher visual resolution (Arrese et al. 2005, Dkhissi-Benyahya et al. 2001, Juliusson et al. 1994, Schiviz et al. 2008), such as the visual streak of the rabbit (Famiglietti & Sharpe 1995, Oyster et al. 1981) (**Figure 2*b***), sheep (Shinozaki et al. 2010) (**Figure 2*c***), or giraffe (Coimbra et al. 2013, Schiviz et al. 2008) (**Figure 2*d***). In contrast, the distribution of S opsins greatly varies across mammals (**Figure 2**). Similar to the house mouse (*Mus musculus*) (**Figure 2*a***) and several laboratory mouse strains (Szél et al. 1992), the rabbit (Famiglietti & Sharpe 1995, Juliusson et al. 1994) (**Figure 2*b***), the Chilean subterranean rodent cururo (Peichl et al. 2005), the European mole (Glösmann et al. 2008), the shrew (Peichl et al. 2000), and even the spotted hyena (Calderone et al. 2003) show higher S-opsin expression in the ventral retina. Other species, such as the sheep (Shinozaki et al. 2010) (**Figure 2*c***), goat, and bison (Schiviz et al. 2008), as well as several marsupials (Arrese et al. 2003, 2005; Hemmi & Grünert 1999), display the opposite trend, with higher S-cone opsin density in the dorsal retina. Note that the division based on dorso-ventral S-opsin expression is rough and overly simplified. For example, mouse S opsins are sparse in the dorsal half of the retina and dominate the ventral half of the retina (Applebury et al. 2000, Haverkamp et al. 2005, Nikonov et al. 2006, Szél et al. 1992, Wang et al. 2011, Warwick et al. 2018) (**Figure 2*a***), but in the rabbit, they are sparse throughout the retina except for a narrow band in the most ventral periphery, where they exhibit a high density (an area called the blue streak) (Famiglietti & Sharpe 1995, Juliusson et al. 1994) (**Figure 2*b***). In addition,

certain species have a unique distribution of S opsins. For example, the ground squirrel shows a dramatic increase in S opsins in the extreme dorso-nasal retinal margin (Kryger et al. 1998), and the giraffe's S-cone opsin density is increased in the dorso-temporal retinal area (Schiviz et al. 2008) (**Figure 2*d***). For more examples of intraretinal variability in vertebrate visual pigments, the reader is referred to Temple (2011) and Peichl (2005).

The variations in the topographic distribution of cone opsins may have an evolutionarily adaptive role, optimizing the animal's visual sensitivity and improving its chances of mating and survival. Thus, for a small animal that is under continuous danger of being hunted by birds of prey, the shift in spectral sensitivity toward short wavelengths in the upward-looking ventral retina may enhance contrast of objects against the skylight, which is relatively rich in shortwave components. This is further discussed in Section 5. Larger species may benefit from an overlap of M and S cones in high densities in their downward-looking dorsal retina to enhance color discrimination, which may be useful for food search and orientation within the habitat (Schiviz et al. 2008). Nevertheless, these speculations do not explain numerous exceptions, such as the dense S-opsin expression in the spotted hyena's ventral retina (Calderone et al. 2003) and the high concentration of S opsins in the dorso-temporal retina of the fat-tailed dunnart—a marsupial the size of a mouse (Arrese et al. 2003). Moreover, a large diversity is reported even among different mouse species: the wood mouse (*Apodemus sylvaticus*) exhibits a low density of S opsins with a centroperipheral gradient, while the herb field mouse (*Apodemus microps*) completely lacks S opsins in its retina (Szél et al. 1994). A unique feature was found in a specific outbred strain of the wild house mouse (*M. musculus*) native to Idaho, United States (Chalfin et al. 2014). These mice exhibited a dorso-ventral gradient of S opsins that is similar to that of the lab mouse, but in the ventral retina, their cone photoreceptors formed a regular mosaic of high-density cone clusters. In the dorsal retina, cone photoreceptors were distributed evenly (Warwick et al. 2018).

The unexplained opsin densities of numerous species raise a contradicting hypothesis according to which there is no etiological role for the inhomogeneous topographies of cone opsins, and regional differences merely reflect ancestral stages of visual pigment evolution that serve little or no visual function (Szél et al. 1996, Temple 2011). Nevertheless, a more reasonable (and less disappointing) suggestion would be that each species displays a specific topographic arrangement of cones that is optimally matched to its visual requirements and its sensory–ecological environment (Barlow 1961). This idea is supported by two aquatic vertebrates, in which the spectral sensitivity of photoreceptors nonhomogeneously varies across the retina and beautifully matches the visual requirements of the animal in its habitat. Archerfish use their vision to hunt terrestrial insects using spitting jets of water. They possess dichromatic vision in most retinal areas, except in the ventro-temporal area, where their vision is trichromatic (Temple et al. 2010). This area perfectly matches the visual field where aerial prey within reach is detected, optimizing prey detection against a background of overhanging foliage (Temple et al. 2010). In larval zebrafish, UV cones are most dense in a ventro-temporal region of the retina. This UV-specialized area represents the spatial zone of prey within reach, supporting detection and capture of UV-absorbing microorganisms against the UV-rich background (Zimmermann et al. 2018). Therefore, mapping the spectral contents of specific regions in the animal's field of view and understanding the animal's requirements for mating and survival appear to be central to understanding the functional role of cone topography.

5. ANATOMICAL AND FUNCTIONAL TOPOGRAPHIC VARIATIONS OF THE MOUSE RETINA

The mouse retina has been thought to be relatively homogeneous, lacking a specialized retinal area such as a fovea or area centralis (Dräger & Olsen 1981, Jeon et al. 1998). Below, we focus on

recently found inhomogeneities in the house mouse (*M. musculus*, the most common laboratory mouse species) retina and suggest how these variations, including the above-mentioned cone opsin expression, may benefit various behavioral requirements.

5.1. Topographic Variations in Color Vision

Cones constitute only 3% of the photoreceptors in the mouse retina. These cones comprise two populations: The most abundant cone type (95%) coexpresses S and M opsin, with peak sensitivities to UV (360 nm) and green (508 nm) light, respectively, and a minority of the cones (5%) are true S cones that express only S opsin (Applebury et al. 2000, Haverkamp et al. 2005, Nikonov et al. 2006, Wang et al. 2011). While true S cones are evenly distributed across the retina, coexpressing cones display nonhomogeneous opsin distribution, generating a dorso-ventral gradient in M:S ratio with M opsins dominating the dorsal retina and S opsins dominating the ventral retina. This gradient is slightly tilted, showing increased S-opsin expression earlier along the dorso-ventral axis in the nasal region compared to the temporal region (Szél et al. 1994) (**Figure 2*a***).

The graded opsin expression detected in the mouse retina using immunohistochemistry was demonstrated to have functional implications, as retinal neurons display substantial differences in their chromatic tuning in the dorsal and ventral retinal areas. Cones and bipolar cells are spectrally tuned to green light in the dorsal retina and to UV light in the ventral retina (Baden et al. 2013, Breuninger et al. 2011, Szatko et al. 2019). In line with the chromatic preferences of cones and bipolar cells, RGCs in the dorsal retina exhibit higher sensitivity to green light, whereas those in the ventral retina exhibit stronger sensitivity to UV light (Chang et al. 2013, Ekesten & Gouras 2005, Szatko et al. 2019, Wang et al. 2011). This gradient in spectral sensitivity along the dorso-ventral axis is consistent with data obtained from mouse in vivo ERG measurements (Calderone & Jacobs 1995) and has also been reported at the level of the superior colliculus, a major retinorecipient target (Ekesten & Gouras 2001).

Despite the existence of two cone opsins in the mouse retina, it was questionable whether mice can detect color. Coexpression of M and S opsins is expected to deteriorate color vision, which relies on color opponency via cones of different spectral tunings. Moreover, in the ventral retina, M-opsin expression is diminished as cone expression increases to approximately 95% S opsin (Wang et al. 2011). Nevertheless, color opponent RGCs were reported in mice (Ekesten & Gouras 2005, Stabio et al. 2018), and behavioral experiments confirmed that mice can discriminate colors (Denman et al. 2018, Jacobs et al. 2004). Two mechanisms were reported to support color discrimination in the mouse. Notably, each of the mechanisms generates a neural color code in distinct retinal regions instead of providing homogeneous color-opponent responses across the entire retina.

First, α-like RGCs exhibit color-opponent responses (UV-On/green-Off or green-On/UV-Off) along the horizontal midline of the retina (Chang et al. 2013). This area is called the transitional zone, where the dominant opsin in coexpressing cones changes from M to S opsin. The color opponency of α-RGCs in this region is suggested to arise from their relatively large dendritic arbors, allowing the cells to gather inputs from coexpressing cones that express the two opsins at different levels (Chang et al. 2013). In accordance with this, when the stimulus size decreases, the cell's responses become nonopponent, probably because the stimulating area is too small to recruit both M- and S-opsin-mediated responses (Chang et al. 2013). Second, the receptive field center of JAM-B RGCs, a subtype of Off RGCs (Kim et al. 2008), matches the cone opsin gradient, displaying green-Off center responses in the dorsal and UV-Off center responses in the ventral retina. In contrast, the surround exhibits green-On responses regardless of retinal location (Joesch & Meister 2016). Interestingly, the green-sensitive surround in the S-opsin-dominant

ventral region is mediated by rod photoreceptors, whose spectral sensitivity resembles that of M cones. As a result, JAM-B RGCs located in the ventral retina display color-opponent responses (UV-Off/green-On). This mechanism for color opponency is not restricted to JAM-B RGCs, as cones, bipolar cells, and other RGCs in the ventral retina were shown to have color-opponent responses as well (Szatko et al. 2019). Interestingly, color opponency is largely absent in the dorsal retina (Szatko et al. 2019). Thus, a rod–cone opponent mechanism may support color discrimination in the ventral retina despite the lack of substantial M-opsin expression (Denman et al. 2018, Joesch & Meister 2016, Szatko et al. 2019). The opposing opsin gradients may further influence retinal processing. For example, starburst amacrine cells were shown to switch their polarity preference (from On to Off or vice versa) as a result of repetitive stimulation with light devoid of UV components (Vlasits et al. 2014). This polarity switch was exclusive to the dorsal retina and was suggested to result from changing interactions between rods and cones, appearing when the wavelength of the visual stimulus matches the spectral preference of the cones (Vlasits et al. 2014).

Direction-selective RGCs (DSGCs): RGCs that encode motion, responding maximally to an object moving in one, preferred direction but not in the opposite direction

Intrinsically photosensitive RGCs (ipRGCs): melanopsin-containing RGCs that constitute a third class of photoreceptors, involved in non-image-forming vision

5.2. Anatomical and Functional Topographic Variations in Retinal Ganglion Cells

Apart from the known variation in mouse cone opsins and the consequences that it has on chromatic preference in different retinal regions, the mouse retinal circuitry has been thought to be relatively homogeneous. Distributions of each neuronal class were reported to be largely uniform across the retina, with only a slight decrease in cell density toward the peripheral edges (Dräger & Olsen 1981, Jeon et al. 1998). Among retinal neuronal classes, RGCs show the largest variation in cell density, reaching a maximum of 8,000 cells/mm^2 in the central-ventral retina and a minimum of 2,000 cells/mm^2 in the far dorso-temporal retinal region (Dräger & Olsen 1981, Jeon et al. 1998) (**Figure 3*a, i***). Yet morphological studies did not report on variations in dendritic arbor or soma size with retinal location or eccentricity (Coombs et al. 2006, Sun et al. 2002). As a result, mouse RGC subtypes were often classified based on soma and dendritic arbor size, branching patterns, and stratification layers (Badea & Nathans 2004, Kong et al. 2005, Völgyi et al. 2009). However, the idea that the mouse retina is homogeneous was proven wrong with the use of molecular markers that enable identification of specific RGC subtypes. The mouse retina contains >30 different subtypes of RGCs (Baden et al. 2016). As described below, different RGC subtypes were shown to display distinct density functions, variations in dendritic arbor size and morphology across the retina, and variations in coverage factor (i.e., number of cells that sample any given point in the visual field). Although cell density and dendritic arbor size often vary in an inversely proportional manner to maintain a uniform coverage factor across the retina (Wässle et al. 1981), in some cases, they vary independently, resulting in a nonuniform coverage factor.

On–Off posterior-preferring direction-selective ganglion cells (DSGCs) labeled in the TRHR-GFP mouse line (Rivlin-Etzion et al. 2011) display larger dendritic arbors in the dorsal than in the ventral retina (El-Danaf & Huberman 2019) (**Figure 3*a, ii***). This variation in dendritic arbor size could serve to maintain a uniform coverage factor across the retina, as it inversely matches the density function of these cells, which is higher in the ventral region (Rivlin-Etzion et al. 2011). Unlike the TRHR-DSGCs, M1 and M2 melanopsin-expressing intrinsically photosensitive RGCs (ipRGCs) reveal a higher density and more extensive dendritic networks in the dorsal compared to the ventral retina (Hughes et al. 2013) (**Figure 3*a, iii***). The non-image-forming RGCs that are labeled in the Cdh3-GFP mouse line comprise two subtypes (Osterhout et al. 2011) that have distinct topographies: One subtype (NIF-On RGC) exhibits smaller dendritic arbors in the nasal compared to temporal retina (**Figure 3*a, v***), while the other subtype (NIF-Diving RGC) does not show significant changes in arbor size as a function of retinal location (El-Danaf & Huberman

2019) (**Figure 3*a, vi***). Note, however, that there are no labeled cells in the dorsal retina, but whether this is due to nonuniform labeling or because these cells do not exist in the dorsal retina is unknown. The TYW3 mouse line labels W3 RGCs, which have the smallest dendritic arbors among RGCs and respond preferentially to small, dark stimuli (Zhang et al. 2012). W3 RGCs are nonhomogeneously distributed across the mouse retina, displaying a higher density in the ventral retina and a lower density in dorsal and peripheral retinal areas (**Figure 3*a, iv***). In the ventral region, where the density of W3 RGCs is at its highest, their coverage factor is approximately 4.5.

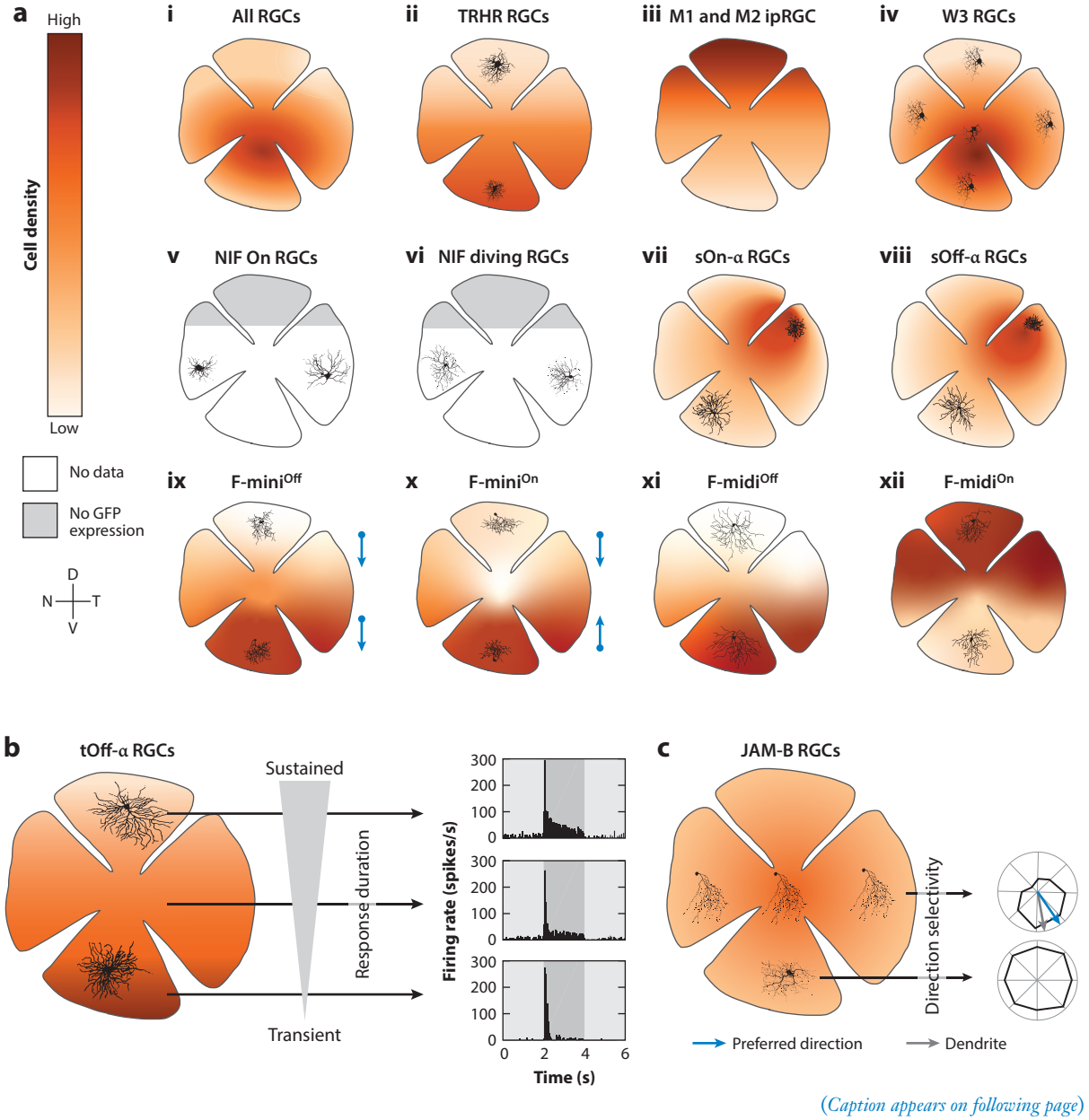

(*Caption appears on following page*)

Figure 3 (*Figure appears on preceding page*)

Variation in density and dendritic arbor size for example mouse retinal ganglion cell (RGC) subtypes. (*a*) Schematic heat maps representing densities of RGC subtypes across the retina (not to scale). Example cell fills or reconstructions are overlain on the approximate retinal location from which they were obtained to illustrate differences in dendritic arbor sizes. For F-mini direction-selective ganglion cells, the preferred direction is represented by a blue arrow next to the retina (*ix* and *x*). Cell fills adapted with permission from El-Danaf & Huberman (2019) (*ii*, *iv*, *v*), Bleckert et al. (2014) (*vii*, *viii*), and Rousso et al. (2016) (*ix–xii*). (*b*) Schematic heat map representing the density of tOff-α RGCs (*left*) and the light responses of three example tOff-α RGCs (peristimulus time histogram in response to a dark spot; *dark bar*) (*right*) taken from three different locations along the dorso-ventral axis (*arrows*). Panel adapted with permission from Warwick et al. (2018). (*c*) Schematic heat map representing the density of JAM-B RGCs (*left*) and the directional tuning of two example JAM-B RGCs (*blue*: directional tuning; *gray*: orientation of dendritic arbor) (*right*) taken from two different locations along the dorso-ventral axis (*arrows*). The upper polar plot was rotated to fit the orientation of dendrites of the example cell. Panel adapted with permission from Kim et al. (2008). To improve visibility, cell fills are not to scale.

Since W3 RGCs have similar dendritic arbor sizes in the ventral and dorsal retina (El-Danaf & Huberman 2019), their reduced density in the dorsal retina and periphery dictates a decrease in coverage factor in these regions.

Transgenic mouse lines not only revealed variations in density and dendritic arbor size, but also demonstrated variations in arborization pattern and function. One example comes from JAM-B RGCs (Kim et al. 2008). Most JAM-B RGCs have asymmetric dendritic arbors pointing ventrally, but near the dorsal and ventral retinal margins, their dendrites are symmetric (**Figure 3*c***). These anatomical variations may have functional implications, as asymmetric JAM-B RGCs respond selectively to stimuli moving in a soma-to-dendrite direction, whereas symmetric JAM-B RGCs show no directional preference (Kim et al. 2008) (**Figure 3*c***). Another example was demonstrated by Rousso and colleagues (2016), who identified a family of RGCs that express the transcription factor Foxp2 (**Figure 3*a*, *ix–xii***). Using intersectional labeling techniques, they divided these RGCs into four subtypes. All four F-RGC subtypes have asymmetric dendrites oriented along the dorso-ventral axis. F-mini^{Off} and F-mini^{On} RGCs have small dendritic arbors and are direction selective, with their preferred direction corresponding to the direction in which their dendrites point. Notably, dendrites of F-mini^{Off} RGCs tend to point ventrally (**Figure 3*a*, *ix***), but the asymmetry of F-mini^{On} RGCs varies with location, with dendrites pointing ventrally in the dorsal retina and dorsally in the ventral retina (**Figure 3*a*, *x***). As a result, all F-mini^{Off} RGCs share the same upward directional preference, whereas F-mini^{On} RGCs display opposing preferred directions, preferring upward motion in the dorsal retina and downward motion in the ventral retina. F-midi^{On} and F-midi^{Off} RGCs are larger and non–direction selective. Both F-mini subtypes and F-midi^{Off} RGCs are denser in the ventral than the dorsal retina, but F-midi^{On} RGCs display the opposite density profile (**Figure 3*a*, *xii***). For all four subtypes, the size of dendritic arbors scales with local density, so that the coverage factor is uniform and independent of retinal location (Rousso et al. 2016).

Other studies investigated topographic variations of α-like RGCs by characterizing their density, their dendritic arbor size, and the distribution of presynaptic partners. Sustained-On-α RGCs (sOn-α RGCs) display a nasal-to-temporal gradient in their density, with a threefold higher density in the temporal than in the nasal retina (Bleckert et al. 2014) (**Figure 3*a*, *vii***). In parallel, dendritic arbor size gradually changes, being largest in the nasal retina and smallest in the highly populated temporal retina. While sOn-α RGCs in both temporal and nasal regions show the characteristic sustained excitatory and inhibitory currents in response to light onset, receptive field sizes of temporal sOn-α RGCs are greater than their dendritic arbor size, but receptive field sizes of nasal sOn-α RGCs match their dendritic arbor size. As a result, the functional coverage of sOn-α RGCs is >2-fold higher in temporal compared to nasal retina (Bleckert et al. 2014). Interestingly, axon sizes of type 6 bipolar cells, a primary excitatory presynaptic neuron to sOn-α RGCs, do not scale

with sOn-α RGC receptive field sizes, but instead show similar axon sizes in nasal and temporal retina (Bleckert et al. 2014). α-RGCs do not necessarily share the same topography: While sOff-α RGCs vary in density and dendritic arbor size, similar to sOn-α RGCs (**Figure 3*a, viii***), transient Off-α RGCs (tOff-α RGCs) do not show the same trend along the naso-temporal axis (Bleckert et al. 2014). Instead, tOff-α RGCs show a moderate decrease in dendritic arbor size, as well as a higher density, in the ventral retina (Warwick et al. 2018, Yu et al. 2018) (**Figure 3*b***), corresponding to the peak density of the entire RGC population (Dräger & Olsen 1981). Investigation of potential presynaptic partners demonstrated that Off bipolar cells can also have topographic variations: Type 1 Off bipolar cells display a constant axon terminal size across the retina, but types 2, 3a, and 4 exhibit smaller terminal sizes in ventral than in dorsal regions (Yu et al. 2018). As a result, while tOff-α RGCs' variation in dendritic arbor size along the ventro-dorsal axis matches the variation in axon terminal size of their main presynaptic partners, type 3a and type 4 Off bipolar cells, the variation of sOff-α RGCs does not parallel their main presynaptic inputs, the type 2 bipolar cells, as these cells vary over orthogonal retinal axes (Yu et al. 2018). Regardless of the matching or nonmatching topographies, the proportion of inputs from bipolar cells to each Off-α RGC type does not change with retinal location, due to a constant density of bipolar cell output synapses, which are independent of axon terminal size (Yu et al. 2018). Thus, the density of synapses from bipolar cells onto OFF-α RGCs is maintained despite topographic changes in the size of bipolar cell or RGC arbors.

A recent study demonstrated that cells belonging to a single RGC subtype can exhibit different response properties depending on their location in the retina, even if they share a similar morphology. Response durations of tOff-α RGCs to a dark stimulus are transient in the ventral region (as one could expect from their name) but gradually become more sustained toward the dorsal retina, revealing >5-fold longer durations of responses in the dorsal region (Warwick et al. 2018) (**Figure 3*b***). These differences in response durations between dorsal and ventral tOff-α RGCs are most apparent under photopic illumination. Yet they do not result from the gradual change in cone opsins, as dorso-ventral differences are found under conditions that preferentially activate the green-sensitive cones as well as under conditions that preferentially activate the UV-sensitive cones. Instead, variations in response duration result from alterations in neural circuits underlying tOff-α RGC responses. tOff-α RGCs gather input from both the cone pathway via Off cone bipolar cells and the primary rod pathway via AII amacrine cells (Manookin et al. 2008, Murphy & Rieke 2008). Under pharmacological blockade of AII cells, tOff-α RGCs revealed similar light responses in dorsal and ventral retina, suggesting that cone inputs do not vary with retinal location. Elimination of the cone signal using mice that lack cone function ($Gnat2^{-/-}$) revealed robust sustained responses in dorsal tOff-α RGCs but only short and diminished responses in ventral tOff-α RGCs. Thus, input from the primary rod pathway via the AII amacrine cells underlies the difference in response duration between tOff-α RGCs in the dorsal and ventral retina. Differences between dorsal and ventral tOff-α RGCs do not result from excessive inbreeding and are not specific to a certain laboratory strain, as they are also found in wild house mice that were trapped in fields and kept under laboratory conditions for a maximum of 10 generations (Warwick et al. 2018).

To conclude, different RGC subtypes display distinct topographies in terms of density and cell morphology. Moreover, some RGC subtypes reveal functional inhomogeneities, qualitatively changing their light responses with retinal location. Whether these differences are unique to the mouse retina or whether the genetic power reveals a concept that is preserved across species remains to be determined, but these differences suggest that the customized distributions of each RGC subtype serve to encode specific visual features encountered in specific regions of the visual field to optimally sample the mouse's visual environment.

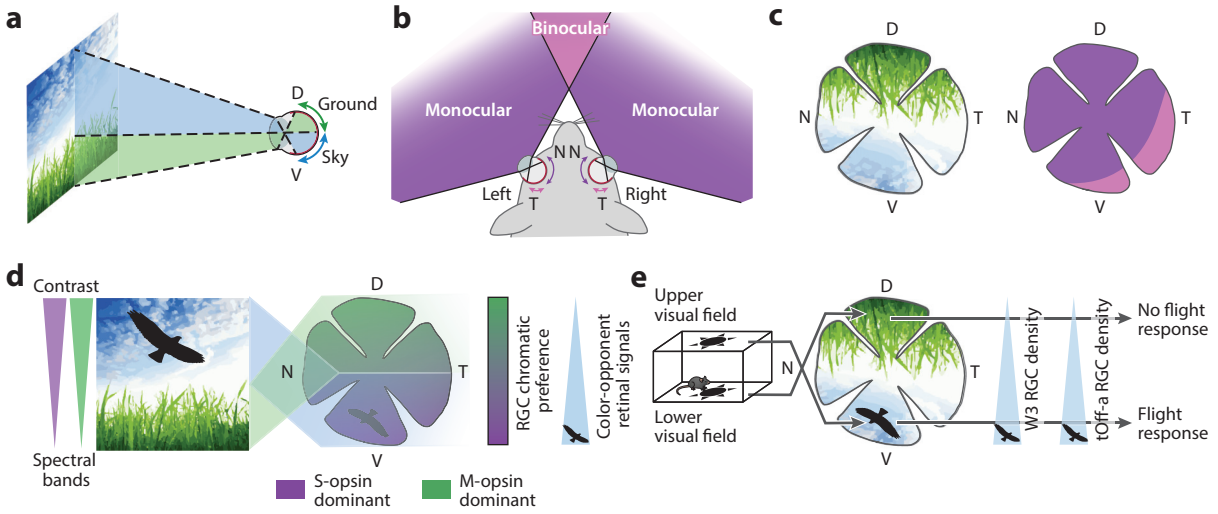

Figure 4

Functional requirements of different retinal areas. (*a*) Schematic representation of the upper (sky) and lower (ground) visual fields on the retina. The dorsal retina views the ground and the ventral retina views the sky. (*b*) Diagram illustrating the separation of monocular and binocular visual fields on the retina. The binocular field of view falls on the temporal retina and the monocular or peripheral field of view on the nasal retina. (*c*) Schematic representation of the retina's view of the visual field (*left*) and of retinal areas that encode monocular and binocular vision (*right*). (*d*, *left*) Diagram illustrating that, in mouse natural visual scenes, the contrasts in the UV and green band are more different in the upper than in the lower visual field. (*Right*) Diagram illustrating the opsin dominance in the mouse retina and the corresponding chromatic preference of retinal ganglion cells (RGCs). Color-opponent signals of all retinal cell types are more abundant in the ventral retina. (*e*) Diagram illustrating an experiment in which a dark looming spot presented in the upper visual field (corresponding to the ventral retina) elicits a flight response, while the same stimulus presented in the lower visual field (dorsal retina) does not. Accordingly, the densities of W3 RGCs and transient Off-α RGCs, two potential candidate cell types for encoding approaching dark objects, are higher in the ventral retina.

5.3. Functional Requirements of Different Retinal Areas

Topographical variations in the retina exist on various levels and include variations in cell density, distribution, and function. But how do these specializations meet the ecological requirements of animals living in the wild? Different retinal areas will be directed at different parts in the visual field, and are therefore expected to encode behaviorally relevant features present in those visual areas. In the mouse, two major axes with ecological relevance can be drawn in the retina. First, as the mouse is a small animal that views the environment from close to the ground, the horizontal axis separates the retinal image into the upper and lower visual fields that primarily correspond to the sky and the ground, falling on the ventral and the dorsal retina, respectively (**Figure 4*a*,*c***). Second, a vertical axis separates the retinal image into the monocular and binocular visual fields, which fall on the nasal and temporal retina, respectively (**Figure 4*b*,*c***).

As described above, spectral tuning of retinal cells changes along the dorso-ventral axis from green to UV, and the ventral retina is more specialized in discriminating color signals than the dorsal retina (**Figure 4*d***). This is in line with analyses of mouse natural scenes, which suggest that contrasts in the UV and green spectral band are more different in the upper than the lower visual field (Y. Qiu, T. Euler, & K. Franke, unpublished observations) (**Figure 4*d***, *left*). Retinal images arising from the upper visual field are mainly concerned with detection of birds of prey, a major predator of mice (Singleton & Krebs 2007). With relatively high levels of UV radiation from the sun, dark moving objects such as birds will result in negative contrast images by occluding UV

light projecting onto the ventral retina. Accordingly, cones in the ventral retina were shown to preferentially encode negative contrasts, whereas cones in the dorsal retina respond with equal amplitude to positive and negative contrasts (Baden et al. 2013). In addition, several subtypes of Off RGCs, as well as On–Off RGCs, are denser in the ventral retina (Rivlin-Etzion et al. 2011, Rousso et al. 2016, Warwick et al. 2018, Yu et al. 2018, Zhang et al. 2012) (**Figure 3**). Specifically, W3 RGCs have small receptive fields and selectively respond to dark moving objects (Zhang et al. 2012). Thus, their higher density in the ventral retina seems ideal for detecting approaching predators in the upper visual field. Another RGC type, the PV-5 cell, which likely corresponds to the tOff-α RGC (Farrow et al. 2013), may also play a role in predator detection, as it shows approach-sensitive responses to dark expanding stimuli (Münch et al. 2009) (**Figure 4*e***). The enhanced color discrimination in the ventral region may further aid the detection of predators under varying light regimes and during different times of the day. However, the dorsal retina views the lower visual field, on which mice mainly rely on for foraging and orientation in their environment. The finding that tOff-α RGCs in the dorsal retina have more sustained responses than those in the ventral retina (Warwick et al. 2018) (**Figure 3*b***) might give the mouse an advantage: During foraging, the sustained responses in the dorsal retina would allow the cells' firing rate to be modulated to both increase and decrease, expanding the diversity of possible responses, whereas a transient response in the ventral retina may be sufficient to provide a fast alarm signal in case of an overhead predator (Warwick et al. 2018). However, whether and to what extent mice rely on their visual system for foraging are unknown. Mice mainly forage at dusk in low light levels and might rely more on olfaction and whisking during foraging and exploration. Thus, while vision is probably the major sense used to survey the upper visual field, it is likely to be of less relevance in the lower visual field, where other senses compensate for the lack of chromatic coding in the dorsal retina.

Other hypotheses about the advantage of UV vision include the detection of urine and feces for intraspecies communication (Joesch & Meister 2016, Tovée 1995) or the detection of fruits and seeds that reflect in the UV spectrum (Tovée 1995). However, both urine traces and potential food can mainly be found in the lower visual field and therefore do not match with the UV dominance in the ventral retina. Interestingly, the Eurasian kestrel, which mainly feeds on the vole, was found to use urine traces to track paths of voles when surveying large areas to search for prey (Viitala et al. 1995). While this hypothesis might therefore not hold for small animals active close to the ground, it certainly is employed by other animals.

Studies in mice and rats revealed specific behaviors that seem to be involved in detection and avoidance of predators in the upper visual field. First, it was found that a dark looming spot stimulus, which may mimic an approaching predator, elicits a rapid flight response when presented above the animal, while no flight response is observed when the stimulus is presented from below or the side (Wallace et al. 2013, Yilmaz & Meister 2013) (**Figure 4*e***). Second, rats were shown to use binocular vision for challenging or crucial visual tasks such as detecting predators: Freely moving rats maintain a binocular overhead visual field by asymmetrically and independently moving both eyes (Wallace et al. 2013). Although this has not been tested, a similar principle may be true in mice, which, like rats, need to avoid birds of prey.

Other topographic variations in RGC may reflect the specialized requirements for binocular versus monocular vision. Mice in the wild were shown to feed on seeds and grains, as well as on invertebrates (Singleton & Krebs 2007, Whitaker Jr. 1966). A study that investigated which sensory modalities are necessary for mouse feeding demonstrated that laboratory mice display a robust prey capture behavior when placed in an arena with a cricket. The authors showed that mice rely mainly on vision, as the time needed for prey capture was significantly increased in the dark (Hoy et al. 2016). Moreover, mice oriented themselves toward the target (Hoy et al. 2016),

possibly to view it in the frontal or even binocular visual field, where stereoscopic vision arises. This way, the retinal image would fall onto the temporal retinal areas (**Figure 4*b***). Higher densities and smaller dendritic arbor sizes, which characterize several RGC subtypes in the temporal retina (e.g., sOn-α, sOff-α) (Bleckert et al. 2014) (**Figure 3*a***), would improve spatial acuity and may therefore be beneficial for visually guided tasks requiring fine spatial resolution in the binocular visual field.

Overall, we seem to encounter a variety of topographic specializations in the mouse retina that likely reflect an adaptation to their ecological niche and behavioral requirements, maximizing their chance of survival in their specific habitat.

6. DISCUSSION

Traditionally, RGCs have been classified into subtypes based on their morphology, their light responses, and the presence of a mosaic tiling. The rationale is simple: Neurons belonging to a single subtype should encode a specific feature and therefore are expected to have similar properties and tile the retina for homogeneous representation of the visual feature across the entire visual field. The discoveries demonstrating location-dependent variations in RGCs' morphology, density, and even function (**Figures 1** and **3**) have challenged this method of classification and suggest that the number of RGC subtypes may have been overestimated. New approaches for cell classification that are based on gene expression patterns or anatomical connectivity further demonstrate that the different criteria do not always agree (Kim et al. 2008, Vlasits et al. 2019, Warwick et al. 2018). Notably, some of the most detailed technologies, like electron microscopy reconstructions, are limited to small retinal areas, and therefore, their results cannot always automatically apply to the entire retinal area. So how should we define a cell subtype in light of the striking topographic variations in the retina? One extreme view may be that, given the topographical variations of various retinal neurons—photoreceptors as well as RGCs—the mosaic notion should be abandoned. Instead, cells should be classified independently in specific retinal regions (e.g., in center, dorsal, and ventral retina). However, since the topographic variations tend to present a gradual change across the retina—usually from center to periphery or along the vertical or horizontal axes—such arbitrary and abrupt separation between retinal regions will likely lead to limited insight. Another possible approach would be to choose one criterion that is most relevant for the research question. For example, one may want to concentrate on the functional output, as this criterion provides the most meaningful information about how the retina works (Vlasits et al. 2019). This approach of emphasizing function may be further specialized: As the animal has different natural visual inputs and behavioral demands in the different visual fields (**Figure 4**), one may want to normalize neuronal function accordingly. For example, assuming that mouse natural visual scenes require higher sensitivity to UV and green light in the upper and lower visual fields, respectively, a functional representation that matches this chromatic requirement on the level of the retina would be considered as homogenous. A recent study demonstrated that the directional preference of DSGCs changes topographically to align with the optic flow patterns produced when the mouse advances or retreats along the body axis, as well as when it rises or falls along the gravitational axis (Sabbah et al. 2017). The approach of normalizing neuronal function to the visual inputs and requirements may be most accurate and explain many of the topographic variations; however, we still lack a comprehensive understanding of the behavioral demands of different species.

Many of the topographic variations found in the mouse retina were made possible by the usage of transgenic mice, which label specific subtypes of retinal neurons. Although such transgenic mice pose some limitations, as cell labeling may not be complete or uniform, other techniques (e.g., immunohistochemistry and cell fills) also demonstrate topographic variations (Bleckert et al.

2014, El-Danaf & Huberman 2019). The inhomogeneities found in the mouse retina suggest that, despite the accepted view, there is an area centralis–like region in the mouse ventral retina. This idea is supported by several findings. First, RGCs are more densely populated in the ventral retina, and density distributions of many RGC subtypes show this tendency (**Figure 3**). Second, the gradient opsin expression along the dorso-ventral axis, supported by rod chromatic tuning, generates color vision in ventral but not dorsal retina (**Figure 4**). Third, some wild mice reveal an organized mosaic of high-density cone clusters that is localized exclusively in the ventral retina (Warwick et al. 2018). Fourth, while objects in the lower visual field may be represented by other senses such as olfaction or whisking, objects in the upper visual field rely mainly on vision for detection (De Franceschi et al. 2016). Consistent with this idea, the non-image-forming M1 and M2 ipRGCs are more densely populated in the dorsal retina.

Topographic variations in the retina may have critical implications for downstream areas. Central visual structures may nonuniformly encode certain visual features viewed in particular locations of the visual field. A prominent example is the fovea, whose area accounts for <1% of the retinal area but that is highly overrepresented in higher visual areas (Azzopardi & Cowey 1993). Moreover, nonmatching variations in receptive field sizes of different RGC subtypes may create distinct and nonmatching retinotopic maps in central visual structures (Seabrook et al. 2017). RGCs project to >40 brain nuclei (Morin & Studholme 2014), and therefore, subtypes of nonmatching topographies could potentially innervate different nuclei. However, most subtypes of RGCs in the mouse innervate the dorsal lateral geniculate nucleus (dLGN) and the superior colliculus, so these areas are inevitably innervated by RGC subtypes of nonmatching topographies. For example, posterior preferring DSGCs and sOn-α RGCs change their dendritic arbor size along the dorso-ventral and the naso-temporal axes, respectively (**Figure 3**). Both subtypes innervate the dLGN and superior colliculus (although with distinct projection patterns) (Ecker et al. 2010, Rivlin-Etzion et al. 2011). As a result, these nuclei probably have a larger area representing posterior motion in the upper visual field, but also a larger area representing information on light increments carried by sOn-α RGCs in the central visual field. Indeed, evidence for nonhomogenous spatial representations of specific visual properties or of specific areas in the visual field has been reported in higher cortical areas (Denman et al. 2017, Garrett et al. 2014, Rhim et al. 2017, Tan et al. 2015). Many studies in visual neuroscience did not consider retinal inhomogeneities and therefore did not report the exact retinal location from which data were collected. The recent findings of topographic variations discussed in this review imply that variations in density, morphology, and even function should be taken into account when studying specific cell subtypes or population neuronal activity, not only in the retina, but also throughout the entire visual system.

DISCLOSURE STATEMENT

The authors are not aware of any affiliations, memberships, funding, or financial holdings that might be perceived as affecting the objectivity of this review.

ACKNOWLEDGMENTS

We thank William Grimes, Shai Sabbah, Noam Sobel, and members of the Rivlin lab for useful comments and discussions. The authors acknowledge support from the I-CORE (51/11), the Minerva Foundation, the ISF Foundation (1396/15), the European Research Council (ERC-StG 757732), Dr. and Mrs. Alan Leshner, the Lubin-Schupf Fund for Women in Science, the Charles and David Wolfson Charitable Trust, and Ms. Lois Pope. A.S.H. was supported by a Minerva

doctoral fellowship. R.A.W. was supported by the Dean of Faculty fellowship at Weizmann Institute of Science. M.R.-E. is incumbent of the Sara Lee Schupf Family Chair.

LITERATURE CITED

Ahnelt PK, Kolb H. 2000. The mammalian photoreceptor mosaic-adaptive design. *Prog. Retin. Eye Res.* 19(6):711–77

Andrade-de-Costa BL, Pessoa VF, Bousfield JD, Clarke RJ. 1989. Ganglion cell size and distribution in the retina of the two-toed sloth (*Choloepus didactylus* L.). *Braz. J. Med. Biol. Res.* 22:223–36

Applebury ML, Antoch MP, Baxter LC, Chun LL, Falk JD, et al. 2000. The murine cone photoreceptor: A single cone type expresses both S and M opsins with retinal spatial patterning. *Neuron* 27(3):513–23

Arrese CA, Oddy AY, Runham PB, Hart NS, Shand J, et al. 2005. Cone topography and spectral sensitivity in two potentially trichromatic marsupials, the quokka (*Setonix brachyurus*) and quenda (*Isoodon obesulus*). *Proc. Biol. Sci.* 272(1565):791–96

Arrese CA, Rodger J, Beazley LD, Shand J. 2003. Topographies of retinal cone photoreceptors in two Australian marsupials. *Vis. Neurosci.* 20(3):307–11

Azzopardi P, Cowey A. 1993. Preferential representation of the fovea in the primary visual cortex. *Nature* 361(6414):719–21

Badea TC, Nathans J. 2004. Quantitative analysis of neuronal morphologies in the mouse retina visualized by using a genetically directed reporter. *J. Comp. Neurol.* 480(4):331–51

Baden T, Berens P, Franke K, Román Rosón M, Bethge M, Euler T. 2016. The functional diversity of retinal ganglion cells in the mouse. *Nature* 529(7586):345–50

Baden T, Osorio D. 2019. The retinal basis of vertebrate color vision. *Annu. Rev. Vis. Sci.* 5:177–200

Baden T, Schubert T, Chang L, Wei T, Zaichuk M, et al. 2013. A tale of two retinal domains: near-optimal sampling of achromatic contrasts in natural scenes through asymmetric photoreceptor distribution. *Neuron* 80(5):1206–17

Barlow HB. 1961. Possible principles underlying the transformations of sensory messages. In *Sensory Communication*, ed. WA Rosenblith, pp. 216–34. Cambridge, MA: MIT Press

Bleckert A, Schwartz GW, Turner MH, Rieke F, Wong ROL. 2014. Visual space is represented by nonmatching topographies of distinct mouse retinal ganglion cell types. *Curr. Biol.* 24(3):310–15

Bowmaker JK, Dartnall HJ. 1980. Visual pigments of rods and cones in a human retina. *J. Physiol.* 298:501–11

Breuninger T, Puller C, Haverkamp S, Euler T. 2011. Chromatic bipolar cell pathways in the mouse retina. *J. Neurosci.* 31(17):6504–17

Bringmann A, Syrbe S, Görner K, Kacza J, Francke M, et al. 2018. The primate fovea: structure, function and development. *Prog. Retin. Eye Res.* 66:49–84

Bumsted K, Hendrickson A. 1999. Distribution and development of short-wavelength cones differ between Macaca monkey and human fovea. *J. Comp. Neurol.* 403(4):502–16

Calderone JB, Jacobs GH. 1995. Regional variations in the relative sensitivity to UV light in the mouse retina. *Vis. Neurosci.* 12(3):463–68

Calderone JB, Reese BE, Jacobs GH. 2003. Topography of photoreceptors and retinal ganglion cells in the spotted hyena (*Crocuta crocuta*). *Brain Behav. Evol.* 62(4):182–92

Calkins DJ, Schein SJ, Tsukamoto Y, Sterling P. 1994. M and L cones in macaque fovea connect to midget ganglion cells by different numbers of excitatory synapses. *Nature* 371(6492):70–72

Chalfin L, Dayan M, Levy DR, Austad SN, Miller RA, et al. 2014. Mapping ecologically relevant social behaviours by gene knockout in wild mice. *Nat. Commun.* 5:4569

Chang L, Breuninger T, Euler T. 2013. Chromatic coding from cone-type unselective circuits in the mouse retina. *Neuron* 77(3):559–71

Chievitz JH. 1889. *Untersuchungen Über die Area Centralis Retinae*. Berlin: Arch. Anat. Physiol.

Coimbra JP, Hart NS, Collin SP, Manger PR. 2013. Scene from above: retinal ganglion cell topography and spatial resolving power in the giraffe (*Giraffa camelopardalis*). *J. Comp. Neurol.* 521(9):2042–57

Collin SP. 2008. A web-based archive for topographic maps of retinal cell distribution in vertebrates. *Clin. Exp. Optom.* 91(1):85–95

Coombs J, van der List D, Wang GY, Chalupa LM. 2006. Morphological properties of mouse retinal ganglion cells. *Neuroscience* 140(1):123–36

Curcio CA, Allen KA. 1990. Topography of ganglion cells in human retina. *J. Comp. Neurol.* 300(1):5–25

Curcio CA, Allen KA, Sloan KR, Lerea CL, Hurley JB, et al. 1991. Distribution and morphology of human cone photoreceptors stained with anti-blue opsin. *J. Comp. Neurol.* 312(4):610–24

Curcio CA, Sloan KR, Kalina RE, Hendrickson AE. 1990. Human photoreceptor topography. *J. Comp. Neurol.* 292(4):497–523

Dacey DM, Crook JD, Packer OS. 2014. Distinct synaptic mechanisms create parallel S-ON and S-OFF color opponent pathways in the primate retina. *Vis. Neurosci.* 31(2):139–51

Dacey DM, Packer OS. 2003. Colour coding in the primate retina: diverse cell types and cone-specific circuitry. *Curr. Opin. Neurobiol.* 13(4):421–27

Dacey DM, Petersen MR. 1992. Dendritic field size and morphology of midget and parasol ganglion cells of the human retina. *PNAS* 89(20):9666–70

De Franceschi G, Vivattanasarn T, Saleem AB, Solomon SG. 2016. Vision guides selection of freeze or flight defense strategies in mice. *Curr. Biol.* 26(16):2150–54

de Monasterio FM, McCrane EP, Newlander JK, Schein SJ. 1985. Density profile of blue-sensitive cones along the horizontal meridian of macaque retina. *Invest. Ophthalmol. Vis. Sci.* 26(3):289–302

Demb JB, Singer JH. 2012. Intrinsic properties and functional circuitry of the AII amacrine cell. *Vis. Neurosci.* 29(1):51–60

Denman DJ, Luviano JA, Ollerenshaw DR, Cross S, Williams D, et al. 2018. Mouse color and wavelength-specific luminance contrast sensitivity are non-uniform across visual space. *eLife* 7:e31209

Denman DJ, Siegle JH, Koch C, Reid RC, Blanche TJ. 2017. Spatial organization of chromatic pathways in the mouse dorsal lateral geniculate nucleus. *J. Neurosci.* 37(5):1102–16

Dkhissi-Benyahya O, Szel A, Degrip WJ, Cooper HM. 2001. Short and mid-wavelength cone distribution in a nocturnal Strepsirrhine primate (*Microcebus murinus*). *J. Comp. Neurol.* 438(4):490–504

Dräger UC, Olsen JF. 1981. Ganglion cell distribution in the retina of the mouse. *Invest. Ophthalmol. Vis. Sci.* 20(3):285–93

Ecker JL, Dumitrescu ON, Wong KY, Alam NM, Chen S-K, et al. 2010. Melanopsin-expressing retinal ganglion-cell photoreceptors: cellular diversity and role in pattern vision. *Neuron* 67(1):49–60

Ekesten B, Gouras P. 2001. Identifying UV-cone responses in the murine superior colliculus. *Vis. Res.* 41(22):2819–25

Ekesten B, Gouras P. 2005. Cone and rod inputs to murine retinal ganglion cells: evidence of cone opsin specific channels. *Vis. Neurosci.* 22(6):893–903

El-Danaf RN, Huberman AD. 2019. Sub-topographic maps for regionally enhanced analysis of visual space in the mouse retina. *J. Comp. Neurol.* 527(1):259–69

Famiglietti EV, Sharpe SJ. 1995. Regional topography of rod and immunocytochemically characterized "blue" and "green" cone photoreceptors in rabbit retina. *Vis. Neurosci.* 12(6):1151–75

Farrow K, Teixeira M, Szikra T, Viney TJ, Balint K, et al. 2013. Ambient illumination toggles a neuronal circuit switch in the retina and visual perception at cone threshold. *Neuron* 78(2):325–38

Field GD, Gauthier JL, Sher A, Greschner M, Machado TA, et al. 2010. Functional connectivity in the retina at the resolution of photoreceptors. *Nature* 467(7316):673–77

Franke K, Berens P, Schubert T, Bethge M, Euler T, Baden T. 2017. Inhibition decorrelates visual feature representations in the inner retina. *Nature* 542(7642):439–44

Garrett ME, Nauhaus I, Marshel JH, Callaway EM. 2014. Topography and areal organization of mouse visual cortex. *J. Neurosci.* 34(37):12587–600

Glösmann M, Steiner M, Peichl L, Ahnelt PK. 2008. Cone photoreceptors and potential UV vision in a subterranean insectivore, the European mole. *J. Vis.* 8(4):23

Goodchild AK, Ghosh KK, Martin PR. 1996. Comparison of photoreceptor spatial density and ganglion cell morphology in the retina of human, macaque monkey, cat, and the marmoset *Callithrix jacchus*. *J. Comp. Neurol.* 366(1):55–75

Govardovskii VI, Röhlich P, Szél A, Khokhlova TV. 1992. Cones in the retina of the Mongolian gerbil, *Meriones unguiculatus*: an immunocytochemical and electrophysiological study. *Vis. Res.* 32(1):19–27

Grimes WN, Baudin J, Azevedo AW, Rieke F. 2018. Range, routing and kinetics of rod signaling in primate retina. *eLife* 7:e38281

Hauzman E, Bonci DMO, Ventura DF. 2018. Retinal topographic maps: a glimpse into the animals' visual world. In *Sensory Nervous System*, ed. T Heinbockel, ch. 5. London: IntechOpen

Haverkamp S, Wässle H, Duebel J, Kuner T, Augustine GJ, et al. 2005. The primordial, blue-cone color system of the mouse retina. *J. Neurosci.* 25(22):5438–45

Hecht S, Verrijp CD. 1933. Intermittent stimulation by light. III. The relation between intensity and critical fusion frequency for different retinal locations. *J. Gen. Physiol.* 17(2):251–68

Hemmi JM, Grünert U. 1999. Distribution of photoreceptor types in the retina of a marsupial, the tammar wallaby (*Macropus eugenii*). *Vis. Neurosci.* 16(2):291–302

Hendrickson A. 2005. Organization of the adult primate fovea. In *Macular Degeneration*, ed. PL Penfold, JM Provis, pp. 1–23. Berlin: Springer

Hirsch J, Curcio CA. 1989. The spatial resolution capacity of human foveal retina. *Vis. Res.* 29(9):1095–101

Hoy JL, Yavorska I, Wehr M, Niell CM. 2016. Vision drives accurate approach behavior during prey capture in laboratory mice. *Curr. Biol.* 26(22):3046–52

Huberman AD, Niell CM. 2011. What can mice tell us about how vision works? *Trends Neurosci.* 34(9):464–73

Hughes A. 1975. A quantitative analysis of the cat retinal ganglion cell topography. *J. Comp. Neurol.* 163(1):107–28

Hughes A. 1977. The topography of vision in mammals of contrasting life style: comparative optics and retinal organisation. In *The Visual System in Vertebrates*, ed. F Crescitelli, pp. 613–756. Berlin: Springer

Hughes S, Watson TS, Foster RG, Peirson SN, Hankins MW. 2013. Nonuniform distribution and spectral tuning of photosensitive retinal ganglion cells of the mouse retina. *Curr. Biol.* 23(17):1696–701

Isaacson JS, Scanziani M. 2011. How inhibition shapes cortical activity. *Neuron* 72(2):231–43

Jacobs GH. 1993. The distribution and nature of colour vision among the mammals. *Biol. Rev. Camb. Philos. Soc.* 68(3):413–71

Jacobs GH, Neitz J. 1989. Cone monochromacy and a reversed Purkinje shift in the gerbil. *Experientia* 45(4):317–403

Jacobs GH, Neitz J, Deegan JF. 1991. Retinal receptors in rodents maximally sensitive to ultraviolet light. *Nature* 353(6345):655–56

Jacobs GH, Williams GA, Fenwick JA. 2004. Influence of cone pigment coexpression on spectral sensitivity and color vision in the mouse. *Vis. Res.* 44(14):1615–22

Jeon CJ, Strettoi E, Masland RH. 1998. The major cell populations of the mouse retina. *J. Neurosci.* 18(21):8936–46

Joesch M, Meister M. 2016. A neuronal circuit for colour vision based on rod-cone opponency. *Nature* 532(7598):236–39

Juliusson B, Bergström A, Röhlich P, Ehinger B, van Veen T, Szél A. 1994. Complementary cone fields of the rabbit retina. *Invest. Ophthalmol. Vis. Sci.* 35(3):811–18

Kim I-J, Zhang Y, Yamagata M, Meister M, Sanes JR. 2008. Molecular identification of a retinal cell type that responds to upward motion. *Nature* 452(7186):478–82

Kolb H, Dekorver L. 1991. Midget ganglion cells of the parafovea of the human retina: a study by electron microscopy and serial section reconstructions. *J. Comp. Neurol.* 303(4):617–36

Kolb H, Marshak D. 2003. The midget pathways of the primate retina. *Doc. Ophthalmol.* 106(1):67–81

Kong J-H, Fish DR, Rockhill RL, Masland RH. 2005. Diversity of ganglion cells in the mouse retina: unsupervised morphological classification and its limits. *J. Comp. Neurol.* 489(3):293–310

Kryger Z, Galli-Resta L, Jacobs GH, Reese BE. 1998. The topography of rod and cone photoreceptors in the retina of the ground squirrel. *Vis. Neurosci.* 15(4):685–91

Lennie P, Haake PW, Williams DR. 1991. The design of chromatically opponent receptive fields. In *Computational Models of Visual Processing*, ed. MS Landy, JA Movshon, pp. 71–82. Cambridge, MA: MIT Press

Levick WR. 1967. Receptive fields and trigger features of ganglion cells in the visual streak of the rabbits retina. *J. Physiol.* 188(3):285–307

Manookin MB, Beaudoin DL, Ernst ZR, Flagel LJ, Demb JB. 2008. Disinhibition combines with excitation to extend the operating range of the OFF visual pathway in daylight. *J. Neurosci.* 28(16):4136–50

Martin PR, Grünert U. 1999. Analysis of the short wavelength-sensitive ("blue") cone mosaic in the primate retina: comparison of New World and Old World monkeys. *J. Comp. Neurol.* 406(1):1–14

Masland RH. 2012. The neuronal organization of the retina. *Neuron* 76(2):266–80

Mauss AS, Vlasits A, Borst A, Feller M. 2017. Visual circuits for direction selectivity. *Annu. Rev. Neurosci.* 40:211–30

Moore BA, Tyrrell LP, Kamilar JM, Collin SP, Dominy NJ, et al. 2017. Structure and function of regional specializations in the vertebrate retina. In *Evolution of Nervous Systems*, ed. J Kaas, pp. 351–72. Amsterdam: Elsevier. 2nd ed.

Morin LP, Studholme KM. 2014. Retinofugal projections in the mouse. *J. Comp. Neurol.* 522(16):3733–53

Moroney MK, Pettigrew JD. 1987. Some observations on the visual optics of kingfishers (Aves, Caraciformes, Alcedinidae). *J. Comp. Physiol. A* 160:137–49

Müller H. 1861. Über das ausgedehnte Vorkommen einer dem gelben Fleck der Retina entsprechenden Stelle bei Thieren. *Naturwiss. Z.* 2:139–40

Münch TA, da Silveira RA, Siegert S, Viney TJ, Awatramani GB, Roska B. 2009. Approach sensitivity in the retina processed by a multifunctional neural circuit. *Nat. Neurosci.* 12(10):1308–16

Murphy GJ, Rieke F. 2008. Signals and noise in an inhibitory interneuron diverge to control activity in nearby retinal ganglion cells. *Nat. Neurosci.* 11(3):318–26

Neitz J, Jacobs GH. 1986. Reexamination of spectral mechanisms in the rat (*Rattus norvegicus*). *J. Comp. Psychol.* 100(1):21–29

Nikonov SS, Kholodenko R, Lem J, Pugh EN. 2006. Physiological features of the S- and M-cone photoreceptors of wild-type mice from single-cell recordings. *J. Gen. Physiol.* 127(4):359–74

Osterhout JA, Josten N, Yamada J, Pan F, Wu S, et al. 2011. Cadherin-6 mediates axon-target matching in a non-image-forming visual circuit. *Neuron* 71(4):632–39

Oyster CW, Takahashi ES, Hurst DC. 1981. Density, soma size, and regional distribution of rabbit retinal ganglion cells. *J. Neurosci.* 1(12):1331–46

Peichl L. 2005. Diversity of mammalian photoreceptor properties: adaptations to habitat and lifestyle? *Anat. Rec. A* 287(1):1001–12

Peichl L, Chavez AE, Ocampo A, Mena W, Bozinovic F, Palacios AG. 2005. Eye and vision in the subterranean rodent cururo (*Spalacopus cyanus*, Octodontidae). *J. Comp. Neurol.* 486(3):197–208

Peichl LEO, Künzle H, Vogel P. 2000. Photoreceptor types and distributions in the retinae of insectivores. *Vis. Neurosci.* 17(6):937–48

Peng Y-R, Shekhar K, Yan W, Herrmann D, Sappington A, et al. 2019. Molecular classification and comparative taxonomics of foveal and peripheral cells in primate retina. *Cell* 176(5):1222–37.e22

Perry VH, Cowey A. 1985. The ganglion cell and cone distributions in the monkey's retina: implications for central magnification factors. *Vis. Res.* 25(12):1795–810

Polyak SL. 1941. *The Retina*. Chicago: Univ. Chicago Press

Polyak SL. 1957. *The Vertebrate Visual System*. Chicago: Univ. Chicago Press

Rhim I, Coello-Reyes G, Ko H-K, Nauhaus I. 2017. Maps of cone opsin input to mouse V1 and higher visual areas. *J. Neurophysiol.* 117(4):1674–82

Rivlin-Etzion M, Grimes WN, Rieke F. 2018. Flexible neural hardware supports dynamic computations in retina. *Trends Neurosci.* 41(4):224–37

Rivlin-Etzion M, Zhou K, Wei W, Elstrott J, Nguyen PL, et al. 2011. Transgenic mice reveal unexpected diversity of on-off direction-selective retinal ganglion cell subtypes and brain structures involved in motion processing. *J. Neurosci.* 31(24):8760–69

Rodieck RW. 1991. The density recovery profile: a method for the analysis of points in the plane applicable to retinal studies. *Vis. Neurosci.* 6(2):95–111

Röhlich P, van Veen T, Szél A. 1994. Two different visual pigments in one retinal cone cell. *Neuron* 13(5):1159–66

Roorda A, Williams DR. 1999. The arrangement of the three cone classes in the living human eye. *Nature* 397(6719):520–22

Rossi EA, Roorda A. 2010. The relationship between visual resolution and cone spacing in the human fovea. *Nat. Neurosci.* 13(2):156–57

Rousso DL, Qiao M, Kagan RD, Yamagata M, Palmiter RD, Sanes JR. 2016. Two pairs of ON and OFF retinal ganglion cells are defined by intersectional patterns of transcription factor expression. *Cell Rep.* 15(9):1930–44

Rovamo J, Raninen A. 1988. Critical flicker frequency as a function of stimulus area and luminance at various eccentricities in human cone vision: a revision of Granit-Harper and Ferry-Porter laws. *Vis. Res.* 28(7):785–90

Sabbah S, Gemmer JA, Bhatia-Lin A, Manoff G, Castro G, et al. 2017. A retinal code for motion along the gravitational and body axes. *Nature* 546(7659):492–97

Schiviz AN, Ruf T, Kuebber-Heiss A, Schubert C, Ahnelt PK. 2008. Retinal cone topography of artiodactyl mammals: influence of body height and habitat. *J. Comp. Neurol.* 507(3):1336–50

Seabrook TA, Burbridge TJ, Crair MC, Huberman AD. 2017. Architecture, function, and assembly of the mouse visual system. *Annu. Rev. Neurosci.* 40:499–538

Seiple W, Holopigian K. 1996. Outer-retina locus of increased flicker sensitivity of the peripheral retina. *J. Opt. Soc. Am. A* 13(3):658–66

Sharpe LT, Stockman A. 1999. Rod pathways: the importance of seeing nothing. *Trends Neurosci.* 22(11):497–504

Shinozaki A, Hosaka Y, Imagawa T, Uehara M. 2010. Topography of ganglion cells and photoreceptors in the sheep retina. *J. Comp. Neurol.* 518(12):2305–15

Singleton GR, Krebs CJ. 2007. The secret world of wild mice. In *The Mouse in Biomedical Research*, Vol. 1, ed. JG Fox, MT Davisson, FW Quimby, SW Barthold, CE Newcomer, AL Smith, pp. 25–51. Amsterdam: Elsevier. 2nd ed.

Sinha R, Hoon M, Baudin J, Okawa H, Wong ROL, Rieke F. 2017. Cellular and circuit mechanisms shaping the perceptual properties of the primate fovea. *Cell* 168(3):413–26.e12

Solomon SG, Martin PR, White AJR, Rüttiger L, Lee BB. 2002. Modulation sensitivity of ganglion cells in peripheral retina of macaque. *Vis. Res.* 42(27):2893–98

Stabio ME, Sabbah S, Quattrochi LE, Ilardi MC, Fogerson PM, et al. 2018. The M5 cell: a color-opponent intrinsically photosensitive retinal ganglion cell. *Neuron* 97(1):150–63.e4

Stone J, Halasz P. 1989. Topography of the retina in the elephant *Loxodonta africana*. *Brain Behav. Evol.* 34(2):84–95

Sun W, Li N, He S. 2002. Large-scale morphological survey of mouse retinal ganglion cells. *J. Comp. Neurol.* 451(2):115–26

Szatko KP, Korympidou MM, Ran Y, Berens P, Dalkara D, et al. 2019. Neural circuits in the mouse retina support color vision in the upper visual field. bioRxiv 745539. **https://doi.org/10.1101/745539**

Szél A, Csorba G, Caffé AR, Szél G, Röhlich P, van Veen T. 1994. Different patterns of retinal cone topography in two genera of rodents, Mus and Apodemus. *Cell Tissue Res.* 276(1):143–50

Szél A, Lukáts A, Fekete T, Szepessy Z, Röhlich P. 2000. Photoreceptor distribution in the retinas of subprimate mammals. *J. Opt. Soc. Am. A* 17(3):568–79

Szél A, Röhlich P. 1992. Two cone types of rat retina detected by anti-visual pigment antibodies. *Exp. Eye Res.* 55(1):47–52

Szél A, Röhlich P, Caffé AR, Juliusson B, Aguirre G, Van Veen T. 1992. Unique topographic separation of two spectral classes of cones in the mouse retina. *J. Comp. Neurol.* 325(3):327–42

Szél A, Röhlich P, Caffé AR, van Veen T. 1996. Distribution of cone photoreceptors in the mammalian retina. *Microsc. Res. Tech.* 35(6):445–62

Tan Z, Sun W, Chen T-W, Kim D, Ji N. 2015. Neuronal representation of ultraviolet visual stimuli in mouse primary visual cortex. *Sci. Rep.* 5:12597

Temple S, Hart NS, Marshall NJ, Collin SP. 2010. A spitting image: specializations in archerfish eyes for vision at the interface between air and water. *Proc. Biol. Sci.* 277(1694):2607–15

Temple SE. 2011. Why different regions of the retina have different spectral sensitivities: a review of mechanisms and functional significance of intraretinal variability in spectral sensitivity in vertebrates. *Vis. Neurosci.* 28(4):281–93

Tovée MJ. 1995. Ultra-violet photoreceptors in the animal kingdom: their distribution and function. *Trends Ecol. Evol.* 10(11):455–60

Tyler CW. 1985. Analysis of visual modulation sensitivity. II. Peripheral retina and the role of photoreceptor dimensions. *J. Opt. Soc. Am. A* 2(3):393–98

Viitala J, Korplmäki E, Palokangas P, Koivula M. 1995. Attraction of kestrels to vole scent marks visible in ultraviolet light. *Nature* 373(6513):425–27

Vlasits AL, Bos R, Morrie RD, Fortuny C, Flannery JG, et al. 2014. Visual stimulation switches the polarity of excitatory input to starburst amacrine cells. *Neuron* 83(5):1172–84

Vlasits AL, Euler T, Franke K. 2019. Function first: classifying cell types and circuits of the retina. *Curr. Opin. Neurobiol.* 56:8–15

Völgyi B, Chheda S, Bloomfield SA. 2009. Tracer coupling patterns of the ganglion cell subtypes in the mouse retina. *J. Comp. Neurol.* 512(5):664–87

Wallace DJ, Greenberg DS, Sawinski J, Rulla S, Notaro G, Kerr JND. 2013. Rats maintain an overhead binocular field at the expense of constant fusion. *Nature* 498(7452):65–69

Walls GL. 1942. *The Vertebrate Eye and Its Adaptive Radiation*. Bloomfield Hills, MI: Cranbrook Inst. Sci.

Wang Y, Macke JP, Merbs SL, Zack DJ, Klaunberg B, et al. 1992. A locus control region adjacent to the human red and green visual pigment genes. *Neuron* 9(3):429–40

Wang YV, Weick M, Demb JB. 2011. Spectral and temporal sensitivity of cone-mediated responses in mouse retinal ganglion cells. *J. Neurosci.* 31(21):7670–81

Warwick RA, Kaushansky N, Sarid N, Golan A, Rivlin-Etzion M. 2018. Inhomogeneous encoding of the visual field in the mouse retina. *Curr. Biol.* 28(5):655–65.e3

Wässle H. 2004. Parallel processing in the mammalian retina. *Nat. Rev. Neurosci.* 5(10):747–57

Wässle H, Grünert U, Röhrenbeck J, Boycott BB. 1989. Cortical magnification factor and the ganglion cell density of the primate retina. *Nature* 341(6243):643–46

Wässle H, Peichl L, Boycott BB. 1981. Dendritic territories of cat retinal ganglion cells. *Nature* 292(5821):344–45

Watanabe M, Rodieck RW. 1989. Parasol and midget ganglion cells of the primate retina. *J. Comp. Neurol.* 289(3):434–54

Waugh SJ, Hess RF. 1994. Suprathreshold temporal-frequency discrimination in the fovea and the periphery. *J. Opt. Soc. Am. A* 11(4):1199–212

Wei W. 2018. Neural mechanisms of motion processing in the mammalian retina. *Annu. Rev. Vis. Sci.* 4:165–92

Whitaker JO Jr. 1966. Food of *Mus musculus*, *Peromyscus maniculatus bairdi* and *Peromyscus leucopus* in Vigo County, Indiana. *J. Mammal.* 47(3):473–86

Williams DR, MacLeod DIA, Hayhoe MM. 1981. Foveal tritanopia. *Vis. Res.* 21:1341–56

Yilmaz M, Meister M. 2013. Rapid innate defensive responses of mice to looming visual stimuli. *Curr. Biol.* 23(20):2011–15

Yu W-Q, El-Danaf RN, Okawa H, Pacholec JM, Matti U, et al. 2018. Synaptic convergence patterns onto retinal ganglion cells are preserved despite topographic variation in pre- and postsynaptic territories. *Cell Rep.* 25(8):2017–26.e3

Zhang Y, Kim I-J, Sanes JR, Meister M. 2012. The most numerous ganglion cell type of the mouse retina is a selective feature detector. *PNAS* 109(36):E2391–98

Zimmermann MJY, Nevala NE, Yoshimatsu T, Osorio D, Nilsson D-E, et al. 2018. Zebrafish differentially process color across visual space to match natural scenes. *Curr. Biol.* 28(13):2018–32.e5